ORIGINAL STUDY

STUDY OF THE STRUCTURE AND PROPERTIES OF ALLOYS OBTAINED BY ELECTROSLAG REMELTING OF STEEL SCRAP ALLOYED WITH CARBIDE-FORMING ELEMENTS

Kenesbekov A[1], Rahimberdinov A[2], Kusainov T[1,*] Karibayeva L[1]

[1] Institute of Composite Materials, Ust-Kamenogorsk 070000, Kazakhstan
[2]Asia Quartz LLP, Ust-Kamenogorsk, Kazakhstan
*Corresponding author: kusainov.temirlan00@mail.ru

Abstract. *This study presents a comprehensive investigation of the effect of plastic deformation on the microstructure, mechanical, tribological, and corrosion properties of an iron-containing alloy produced by the electroslag remelting (ESR) process. The study focused on two states of the material: as-cast after ESR and deformed after subsequent rolling (ESR-R). Using X-ray fluorescence and X-ray diffraction analysis, as well as electron microscopy, the characteristics of the alloy's phase composition and microstructure were determined. It was shown that plastic deformation leads to grain refinement, an increase in defect density, and the formation of secondary phases. A significant increase in the microhardness and wear resistance of the material after rolling was observed, accompanied by a decrease in the coefficient of friction. At the same time, an increase in corrosion current density and corrosion rate was observed, despite a shift of the corrosion potential toward a more positive region. The results obtained indicate the complex nature of the effect of plastic deformation on the alloy's service properties and the need to account for the material's structural state during its application. Translated with DeepL.com (free version).*

Keywords: electroslag remelting, plastic deformation, alloy microstructure, microhardness, tribological properties, corrosion resistance, iron-based alloys.

1. Introduction

One of the most productive and effective methods currently available is the electroslag remelting process, which produces high-quality metallic materials with low levels of non-metallic impurities and enhanced structural uniformity.

The essence of this process lies in remelting the consumable electrode in a bath of molten electrically conductive slag placed in a water-cooled mold, where heat is generated by Joule heating [1]. This mechanism allows for control over the melting of the electrode and the direction of ingot crystallization, which in turn enables the production of metal with a specified macro- and microstructure [2].

ESHP offers a number of advantages, the main one being the presence of a slag bath, which acts as a filtering and refining medium. The metal passes drop by drop through a layer of molten slag, where non-metallic inclusions are removed, alloying elements are redistributed, and the content of harmful impurities is reduced [2, 3]. This process helps to increase the purity of the metal and improve its performance properties [4]. The production of a high-quality ingot essentially depends on factors such as heating rate, the technological parameters of the electric arc melting process, and the thermal conditions during solidification [3, 5]. Deviations from optimal operating conditions can lead to the formation of defects, such as liquidation inhomogeneities and gas contamination, which negatively affect the material's properties [5].

The ESR method has become widely used in the production of structural, tool, stainless, and heat-resistant steels, as well as iron- and nickel-based alloys, for which high structural uniformity and minimal defect content are critical [4, 6]. Historically, the technology was developed in the mid-20th century and was further advanced

Received 15 June 2026; revised 16 June 2026; accepted 20 June 2026.
Published online 24 June 2026

DOI: https://doi.org/10.66310/JPBS3543

thanks to the work of the scientific school associated with E.O. Paton and B.E. Paton, which facilitated its industrial implementation [7,8].

Despite the high quality of the metal after electroslag remelting, the as-cast state of the alloy is characterized by a dendritic structure and microsegregation of alloying elements [3,9]. The presence of such structural features can have a significant impact on the mechanical, tribological, and corruption properties of the material, especially when operated in aggressive environments containing chloride ions [10].

The corrosion resistance of metallic materials is a critical factor determining their durability and reliability. Even minor structural inhomogeneities can initiate the localization of electrochemical processes, leading to the development of pitting and crevice corrosion [10,11]. Consequently, there is a need for additional processing of the material to improve its microstructure.

One effective method for modifying the structure after ESR is plastic deformation, specifically rolling. As a result of the deformation process, grain refinement, phase redistribution, a reduction in chemical heterogeneity, and an increase in the density of crystal lattice defects occur [9,12]. These changes lead to an increase in the material's hardness and strength properties, and also affect its tribological behavior [12].

At the same time, an increase in dislocation density and residual stresses can have an ambiguous effect on corrosion properties. On the one hand, improved structural homogeneity contributes to the formation of a more stable passive layer; on the other hand, increased defect density can accelerate electrochemical metal dissolution processes [11,13].

Thus, the effect of plastic deformation on the performance properties of alloys produced by the electroslag remelting process is complex in nature and requires detailed investigation. Establishing the relationship between structural changes and alterations in mechanical, tribological, and corrosion characteristics is a pressing scientific challenge.

The aim of this work is to investigate the effect of plastic deformation on the structure, mechanical, tribological, and corrosion properties of an iron-containing alloy produced by electroslag remelting, as well as to establish the patterns of change in its characteristics during the transition from the as-cast state to the deformed state.

2. Materials and Methods

2.1 Materials and sample preparation

The investigated material was a Fe-based alloy produced by electroslag remelting (ESR). Two structural conditions of the same alloy were studied:

1. the alloy after electroslag remelting in the as-cast condition (denoted as ESR);
2. the same alloy after ESR followed by plastic deformation by rolling (denoted as ESR-R).

The alloy contained Fe as the main component (>90 wt.%) with alloying additions including Cr, Ni, Ti, and Mo. These alloying elements were selected due to their potential influence on mechanical, tribological, and corrosion properties.

The rolled samples were obtained by plastic deformation of the ESR alloy under controlled rolling conditions. Prior to characterization, all specimens were mechanically ground and polished according to standard metallographic preparation procedures.

2.2 Chemical composition analysis

The chemical composition of the investigated alloy was determined by X-ray fluorescence (XRF) analysis using a portable Hitachi analyzer operating in PQA mode. The measurement time was 10 s for each acquisition. Measurements were performed at two different locations on the sample surface, and the obtained values were averaged. The elemental concentrations were expressed in weight percent (wt.%).

2.3 Phase composition analysis

Phase and structural characterization of the alloy was carried out by X-ray diffraction (XRD) using an X'Pert PRO diffractometer (PANalytical, Netherlands) with Cu Kα radiation.

The diffraction measurements were performed under the following conditions:

- tube voltage: 40 kV;
- tube current: 30 mA;
- scanning step: 0.02°;
- counting time: 1 s per step;
- scanning range: 2θ = 20–90°.

The obtained diffraction patterns were analyzed using HighScore software combined with the PDF-4 crystallographic database.

2.4 Microstructural characterization

The microstructure of the investigated alloys was studied by scanning electron microscopy (SEM) in both secondary electron (SE) and backscattered electron (BSE) imaging modes.

Elemental distribution and local chemical composition were analyzed using energy-dispersive X-ray spectroscopy (EDS) combined with elemental mapping. The analysis was performed for both ESR and ESR-R conditions in order to evaluate the influence of rolling deformation on structural homogeneity and elemental redistribution.

2.5 Mechanical characterization

2.5.1 Vickers microhardness

Vickers microhardness measurements were performed using a load corresponding to the HV0.1 scale. The indentation imprints were analyzed and averaged values were calculated for each structural condition.

2.5.2 Instrumented indentation

Instrumented indentation tests were carried out using a FISCHERSCOPE HM2000 system based on the dynamic indentation method according to DIN EN ISO 14577-1.

The tests were performed using a Vickers diamond indenter with an angle of 136° between opposite faces. The loading range was 0.1–2000 mN, while the indenter approach speed was 2 μm/s. The displacement resolution of the instrument was 0.1 nm.

The following parameters were determined:

- Martens hardness (HM);
- nanohardness;
- elastic modulus.

Experimental data processing was performed using WIN-HCU software.

2.5.3 Rockwell hardness

Additional hardness measurements were carried out using the Rockwell B scale (HRB) to evaluate the macroscopic hardness behavior of the investigated alloy states.

2.6 Tribological testing

Tribological behavior was evaluated using a TRB3 tribometer (Anton Paar Srl, Switzerland) under dry sliding conditions according to the ball-on-disk method described in ASTM G99.

A 3 mm diameter 100Cr6 steel ball was used as the counterbody. The testing conditions were as follows:

- normal load: 15 N;
- sliding speed: 3 cm/s;
- wear track radius: 4 mm;
- sliding distance: 200 m.

The tribological performance was evaluated based on the friction coefficient, wear track morphology, wear track cross-sectional area, and wear rate.

2.7 Scratch testing

Scratch tests were performed to evaluate the deformation and damage behavior of the investigated alloy under progressive loading conditions. During the tests, the friction force, penetration depth, residual depth, and acoustic emission signals were continuously recorded.

The obtained data were used to analyze the resistance of the material against local mechanical damage and crack initiation.

2.8 Electrochemical corrosion testing

Electrochemical corrosion behavior was investigated using a CorrTest CS300M potentiostat/galvanostat.

The tests were carried out in a 3.5 wt.% NaCl solution at 25 °C using a conventional three-electrode electrochemical cell consisting of:

- working electrode: investigated alloy sample with an exposed area of 0.64 cm^2;
- reference electrode: Ag/AgCl;
- counter electrode: platinum electrode.

Potentiodynamic polarization measurements were performed to determine the corrosion potential (Ecorr) and corrosion current density (Icorr). The corrosion parameters were calculated using the Tafel extrapolation method.

3. Results and Discussion

3.1 Chemical composition analysis (XRF)

The chemical composition of the investigated alloy in the as-cast condition after electroslag remelting (ESR) and after subsequent rolling (ESR-R) was determined by XRF analysis. The results are presented in Table 1. The material is a multicomponent Fe-based alloy containing Cr, Ni, Ti, and Mo as the main alloying elements. In both conditions, Fe is dominant and exceeds 90 wt.%.

The detected alloying elements may contribute to improved mechanical, tribological, and corrosion-related properties. Cr and Ni can improve corrosion resistance, Mo may enhance resistance to localized corrosion, while Ti and V may participate in the formation of strengthening phases.

The slight differences in elemental contents between the ESR and ESR-R samples are most likely related to local chemical heterogeneity, surface condition, and the XRF measurement area, rather than to changes in the bulk composition caused by rolling. Overall, XRF analysis confirmed the Fe-based nature of the alloy and the presence of functional alloying additions.

Table 1. Chemical composition of the ESR and ESR-R alloys determined by XRF analysis.

Element	ESR alloy, wt.%	ESR-R alloy, wt.%
Fe	93.47 ± 0.02	91.35 ± 0.73
Cr	2.05 ± 0.01	2.33 ± 0.15
Ni	1.66 ± 0.02	3.13 ± 0.52
Ti	1.15 ± 0.03	1.38 ± 0.01
Mo	0.49 ± 0.00	0.62 ± 0.02
V	0.15 ± 0.003	0.18 ± 0.006
Cu	0.08 ± 0.005	0.14 ± 0.01
Co	0.05 ± 0.01	0.03 ± 0.03
Nb	0.01 ± 0.001	—
W	—	0.02 ± 0.017
As	—	0.02 ± 0.001

3.2 Phase composition and structural analysis (XRD)

Fig. 1 shows the XRD patterns of the alloy in the ESR and ESR-R conditions. In the initial ESR state, the diffraction pattern is dominated by intensive peaks corresponding to the α-Fe crystalline phase. The main reflections located at 2θ ≈ 44–45°, 65°, and 82° correspond to the (110), (200), and (211) crystallographic planes, respectively. The relatively narrow and symmetric diffraction peaks indicate a coarse-grained structure with a comparatively low level of internal stresses.

After plastic deformation by rolling (ESR-R condition), a significant modification of the diffraction pattern is observed. In addition to α-Fe reflections, additional peaks associated with oxide phases (Fe_2O_3 and Fe_3O_4), as well as possible carbide and intermetallic compounds such as Fe_3C, are detected. Moreover, noticeable peak broadening and slight peak shifts are observed, indicating grain refinement, increased dislocation density, lattice distortion, and the formation of residual stresses.

The broadening of diffraction peaks after rolling is associated with strain hardening and accumulation of crystal lattice defects during plastic deformation. The appearance of secondary phases may be related to redistribution of alloying elements and activation of diffusion processes during rolling.

Thus, the XRD analysis demonstrates that the transition from the cast ESR condition to the deformed ESR-R state is accompanied by substantial structural transformation involving grain refinement, increased defect density, and secondary phase formation, which significantly affects the mechanical, tribological, and corrosion properties of the alloy.

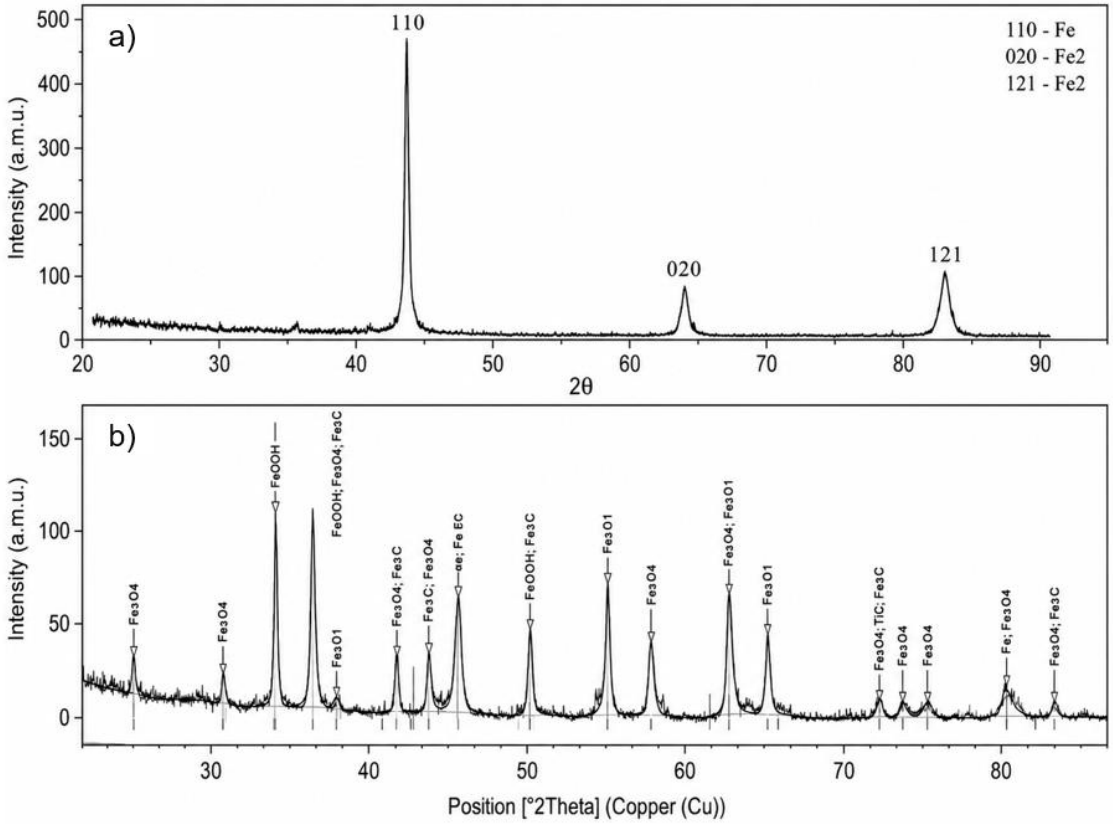

Fig. 1. XRD patterns of the investigated alloy in the ESR and ESR-R conditions.

3.3 Microstructure and elemental distribution (SEM/EDS)

SEM micrographs and EDS elemental mapping results for the alloy in the ESR condition are presented in Fig. 2. The microstructure is characterized by structural heterogeneity with the presence of bright and dark regions corresponding to different phases and inclusions. Elemental mapping confirms that Fe is uniformly distributed within the matrix, while localized regions enriched with Cr, Ni, Mn, and Si are also observed.

Certain inclusions demonstrate enrichment in Ti, V, and Mo, indicating the possible formation of carbide or intermetallic phases. The observed chemical heterogeneity suggests the preservation of segregation effects typical for cast materials after electroslag remelting.

Following rolling deformation (Fig. 3), the microstructure becomes more oriented and homogeneous. The Fe-based matrix demonstrates a more uniform elemental distribution, while alloying elements are dispersed more evenly throughout the material. In addition, the size and frequency of local segregated regions are reduced, indicating a decrease in chemical heterogeneity after plastic deformation.

The obtained results suggest that rolling contributes to structural homogenization and redistribution of alloying elements within the alloy matrix.

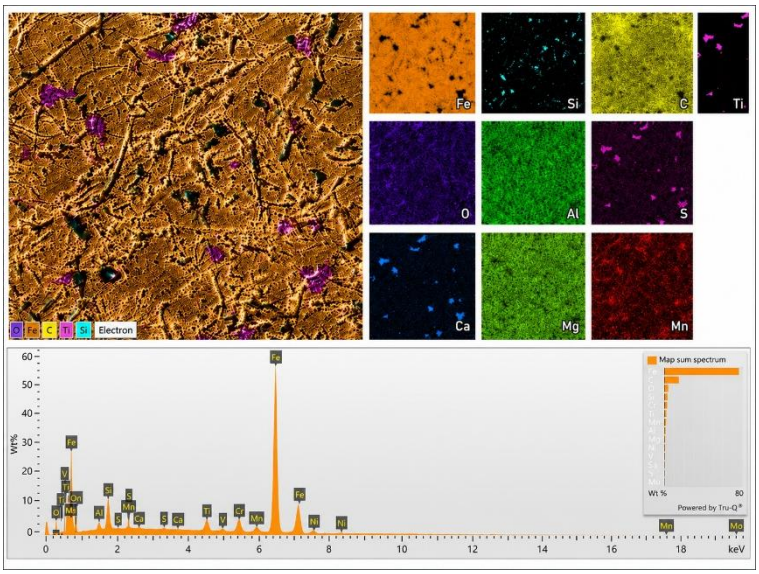

Fig. 2. SEM image and EDS elemental mapping of the alloy in the ESR condition.

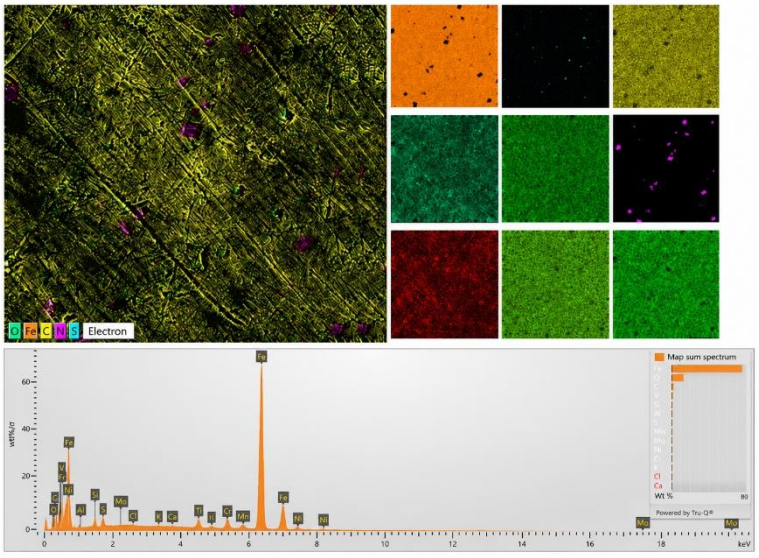

Fig. 3. SEM image and EDS elemental mapping of the alloy in the ESR-R condition.

3.4 Mechanical properties and indentation behavior

3.4.1 Microhardness

Fig. 4 shows the Vickers microhardness results for the investigated alloy. In the ESR condition, relatively large indentation imprints are observed, corresponding to a lower hardness level. The average microhardness value is approximately 394 $HV_{0.1}$.

After rolling deformation (ESR-R), a substantial reduction in indentation size is observed, indicating increased resistance to localized plastic deformation. The average microhardness increases to approximately 914 $HV_{0.1}$, which is more than twice the value of the initial ESR condition.

The observed strengthening effect is mainly associated with grain refinement and increased dislocation density caused by plastic deformation. According to the Hall–Petch mechanism, grain refinement leads to enhanced resistance against dislocation motion, thereby increasing hardness and strength.

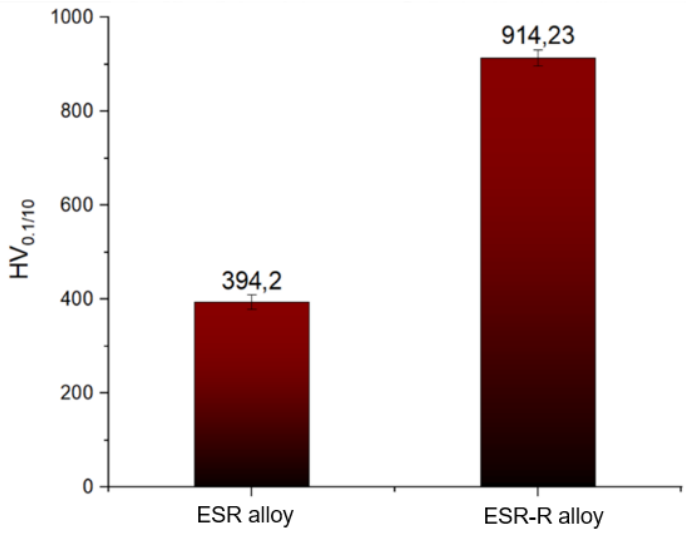

Fig. 4. Vickers microhardness values of the alloy in the ESR and ESR-R conditions.

3.4.2 Instrumented indentation

Additional instrumented indentation tests were performed to determine Martens hardness (HM), nanohardness, and elastic modulus values (Fig. 5). The ESR sample exhibits HM values of approximately 4500 N/mm² and nanohardness values of about 600–650 HV, while the elastic modulus is approximately 236–237 GPa.

After rolling, the HM values increase significantly to approximately 7400–7500 N/mm², whereas nanohardness reaches 1100–1150 HV. In contrast, the elastic modulus changes only slightly and remains within 228–229 GPa.

The obtained hardness values are in good agreement with the Vickers microhardness measurements, confirming the reliability and consistency of the experimental results.

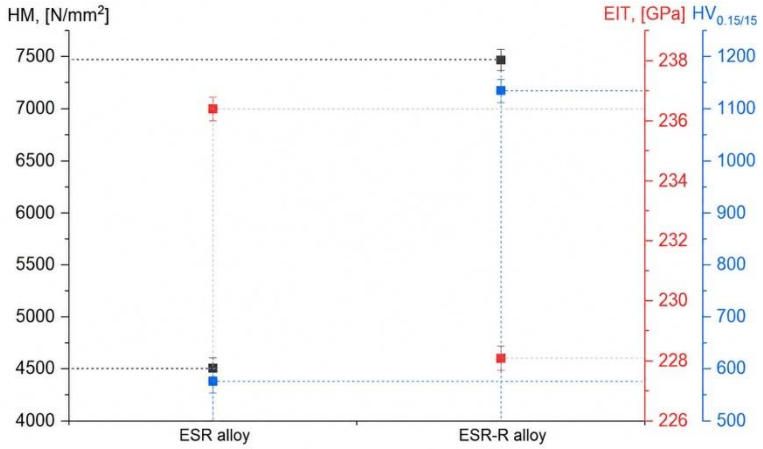

Fig. 5. Instrumented indentation results for the alloy in the ESR and ESR-R conditions.

3.5 Tribological behavior

3.5.1 Friction coefficient

The friction coefficient curves obtained using the ball-on-disk method (ASTM G99) are presented in Fig.6. In both cases, the friction coefficient stabilizes after the running-in stage. However, the ESR sample demonstrates a higher average friction coefficient (~0.65) compared to the ESR-R sample (~0.59).

The reduction in friction coefficient after rolling indicates lower wear intensity and more stable friction behavior. The improved tribological performance is associated with increased hardness and structural homogenization after plastic deformation.

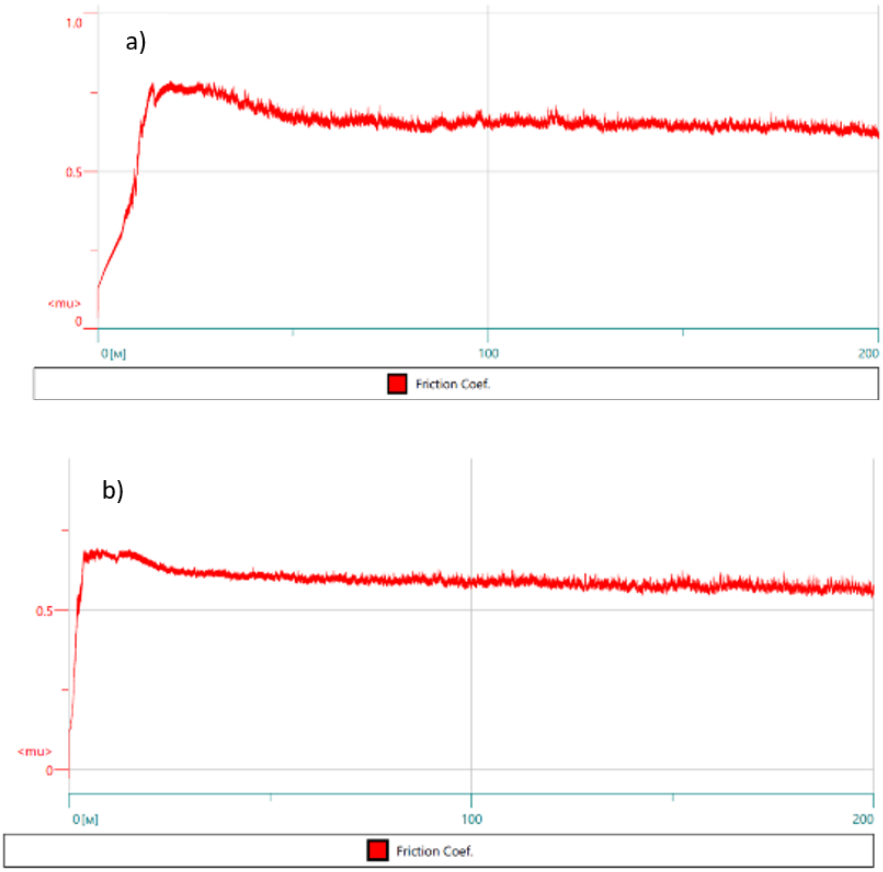

Fig. 6. Friction coefficient as a function of sliding distance for the ESR and ESR-R samples.

3.5.2 Wear track morphology and wear resistance

Wear track surface profiles obtained after tribological testing are shown in Fig. 8. The ESR sample exhibits a wider and deeper wear track with pronounced surface relief changes, indicating severe material removal and intensive plastic deformation during sliding.

In contrast, the ESR-R sample demonstrates a narrower and smoother wear profile with significantly lower wear depth. The cross-sectional wear area decreases from 2528.3 μm² for the ESR sample to 621.7 μm² for the ESR-R sample, corresponding to an approximately 4.1-fold reduction.

Simultaneously, the wear rate decreases from 1.588×10^{-5} to 3.906×10^{-6} mm³/(N·m). The improved wear resistance is attributed to strain hardening, increased hardness, and enhanced structural uniformity of the rolled material.

4. Conclusion

This study investigates the effect of plastic deformation on the microstructure, mechanical, tribological, and corrosion properties of an alloy produced by the electroslag remelting (ESR) process.

It has been established that plastic deformation leads to a significant change in the material's microstructure: grain refinement, an increase in defect density, and a more uniform distribution of alloying elements are observed. This is accompanied by a significant increase in microhardness and an improvement in tribological characteristics, including a reduction in the coefficient of friction and wear rate.

It has been shown that the deformed state is characterized by higher hardness and resistance to local penetration; however, the increase in defect density contributes to increased brittleness and higher electrochemical activity of the material. Electrochemical studies in a NaCl solution confirmed an increase in the rate of corrosion processes following plastic deformation.

Thus, plastic deformation has a complex effect on the properties of the alloy under study: it promotes hardening and increased wear resistance, but simultaneously reduces corrosion resistance. The results obtained can be used in selecting operating conditions and developing processing technologies for materials produced by the ESR method.

Funding

This work does not receive any funding.

Conflict of interest

The authors declare that they have no competing interests.

References

1. Platonov A.D., Gurevich S.M. (1985) Electroslag Remelting of Metals. Moscow: Metallurgiya.
2. Kozlov V.A., Shapovalov V.A. (1990) Theory and Technology of Electroslag Remelting. Moscow: Metallurgiya.
3. Medovar B.I. (1974) Electroslag Remelting. Kyiv: Naukova Dumka.
4. Paton B.E., Medovar B.I. (1991) Electroslag Remelting and Casting. CRC Press.
5. Mitchell A., Smailer R.M. (1979) Practical Aspects of Electroslag Remelting Technology. International Metals Reviews. 24(1), 231–264. https://doi.org/10.1179/imtr.1979.24.1.231
6. Dilthey U., Stein L. (2003) Electroslag Remelting Process: Fundamentals and Applications. Steel Research International.
7. Knyazev M.I., Lysenko A.A. (2001) Metallurgical Processes during Electroslag Remelting. Moscow: Mashinostroenie.
8. Holzgruber H., Steineder K. (2007) ESR Technology for High-Performance Steels. BHM Berg- und Hüttenmännische Monatshefte.
9. Ghosh A., Chatterjee A. (2008) Ironmaking and Steelmaking: Theory and Practice. PHI Learning.
10. Kablov E.N., Lukin A.I. (2012) Modern Technologies for Producing High-Quality Alloys. VIAM.
11. Li J., Thomas B.G. (2004) Modeling of Electroslag Remelting Process. Metallurgical and Materials Transactions B.
12. Wang Q., Zhang L. (2010) Inclusion Removal during Electroslag Remelting. Journal of Materials Processing Technology.
13. Kelkar K.M., Mok J., Patankar S.V., Mitchell A. (2004) Computational Modeling of Electroslag Remelting Processes. Journal de Physique IV France. 120, 325–332. https://doi.org/10.1051/jp4:2004120048
14. Zhukov A.A., Popov V.I. (2006) Special Methods of Metal Melting and Refining. Moscow: Metallurgiya.

AUTHORS' INFORMATION

Kenesbekov Aidar Bakytbekuly - PhD, Director of the Institute of Composite Materials LLP, Ust-Kamenogorsk, Kazakhstan; ORCID iD 0000-0002-5630-9467 (e-mail: aidar.94.01@mail.ru)

Rahimberdinov Askar Olzhaevich - Project Manager at Asia Quartz LLP, Ust-Kamenogorsk, Kazakhstan (e-mail: Askar@asiaquartz.kz)

Kusainov Temirlan Kairatovich - PhD student in Metallurgy, D. Serikbayev East Kazakhstan Technical University, Ust-Kamenogorsk, Kazakhstan; Master of Technical Sciences in Metallurgy; Junior Researcher at the Institute of Composite Materials LLP, Ust-Kamenogorsk, Kazakhstan; ORCID iD 0009-0006-3734-268X (e-mail: kusainov.temirlan00@mail.ru)
Karibayeva Limara Sanatovna - Bachelor student, Junior researcher at the Institute of Composite Materials LLP, Ust-Kamenogorsk, Kazakhstan; ORCID: 0009-0001-6091-1071 (e-mail: limarakairbaeva52@gmail.com)